J Bras Pneumol. 2018;44(6):525-528
http://dx.doi.org/10.1590/S1806-37562018000000080

Near-fatal pulmonary embolism: capnographic perspective

Marcos Mello Moreira[1,2,a], Luiz Claudio Martins[3,b], Konradin Metze[4,c], Marcus Vinicius Pereira[2,d], Ilma Aparecida Paschoal[1,e]

DEAR EDITOR,

Massive pulmonary embolism (MPE) is a condition that causes sudden changes to the cardiopulmonary system[1-5] and is associated with high morbidity and mortality. Methods that detect those changes in real time, especially noninvasive ones, can be very useful. They can also indicate whether the MPE is likely to improve or not.

To address the clinical scenario of MPE, one may make use of noninvasive devices with software that monitors respiratory mechanics and volumetric capnography (VCap) data, online and offline, providing information that may indicate ventilation-perfusion mismatch, in MPE or in other diseases.

The respiratory profile monitor (CO_2SMO PLUS DX-8100; Respironics, Murrysville, PA, USA) provides and records variables such as end-tidal partial pressure of CO_2 ($PetCO_2$), CO_2 output (VCO_2), the phase II slope of the capnogram (SII), the phase III slope of the capnogram (SIII)—also known as the alveolar plateau, respiratory rate (RR), inspiratory tidal volume (V_{Ti}), expiratory tidal volume (V_{Te}), inspiratory time, expiratory time, alveolar minute volume (MValv), peak inspiratory flow, and peak expiratory flow.

This was an observational study of pigs induced to MPE through the injection of autologous clots, during spontaneous ventilation (FiO_2 = 0.21). Our aim was to record, observe, and analyze the behavior of respiratory mechanics parameters, especially VCap data.

We evaluated numerical variables (Table 1) and curves (Figures 1A, 1B, and 1C).

This study was conducted in conjunction with the work published by Pereira et al.,[3] which has been approved by the Ethics Committee on the Use of Animals of the State University at Campinas Institute of Biology (Reference no. 2298-1).

At baseline (T_0, before the clots were injected), all of the variables were measured. The clots were injected in increments of 5 mL until a borderline (i.e., "near-fatal") mean pulmonary artery pressure (the primary endpoint) was reached. The mean quantity of clots injected was 24.7 ± 4.3 mL, and the mean clot injection time was 45 min. As can be seen in Table 1, gas exchange ($PaCO_2$) and hemodynamic changes (cardiac output) were evaluated at three different time points: T_1 (the endpoint), T_2 (30 min after T_1), and T_3 (1 h after T_1).

For the comparison between hemodynamic, gas exchange, and respiratory variables at T_0, T_1, T_2, and T_3, we used repeated-measures ANOVA (Winstat, version 3.1). Values of $p < 0.05$ were considered statistically significant.

$PetCO_2$, MValv, and the alveolar dead space volume presented significant differences among the various time points evaluated, whereas RR did not. It is well known that MPE leads to an increase in RR and in lung volumes. The increase in RR and in lung volumes can be evidenced by a significant increase in MValv, which, in turn, leads to alveolar washout and, as a consequence, to a significant decrease in $PetCO_2$. Another factor that contributed to the reduction in $PetCO_2$ was a significant decrease in pulmonary perfusion (resulting from a decrease in cardiac output). There was a significant increase in the volume of the alveolar dead space, which does not take part in gas exchange. Following the rationale of this variable behavior, the volumes of VCap phases I and II were obtained in mL and per respiratory cycle. Those volumes increased significantly over the study period.

Other variables were provided by VCap or associated with other variables: VCO_2; SII; SIII; VCO_2/V_{Te}; alveolar VCO_2/V_T; SII/exhaled CO_2 partial pressure (SII/P_ECO_2); $SIII/P_ECO_2$; $SIII/PetCO_2$; and $SIII/V_{Te}$. The expected decrease in VCO_2 at T_1 ($p < 0.001$ vs. T_0) can be attributed to the increase in MValv, as well as to a significant reduction in pulmonary blood flow (resulting from a decrease in cardiac output). There were also significant reductions in other metabolic variables, such as VCO_2/V_{Te}, and alveolar VCO_2/V_T.

With similar pathophysiologies, SII and SIII variables also presented significant variations ($p < 0.0001$). The SII represents removal of CO_2 from the alveoli, which are the most distal elements of the small airways. The SIII represents the elimination of CO_2 from most alveoli and, in normal organisms, its shape is similar to a plateau, with a slight upward slope. Higher $SIII/V_{Te}$ and $SIII/PetCO_2$ values suggest structural damage in the peripheral and distal part of the lungs, which promotes this heterogeneous distribution of ventilation.[5,6] The same principle applies to the significant drop in the normalization of SII/P_ECO_2, $SIII/P_ECO_2$, $SIII/PetCO_2$, and $SIII/V_{Te}$ ($p < 0.0001$ for all). Negative SIII values seem to be associated with vascular damage,[2,5] whereas an excessive increase in these values may be associated with airway damage

1. Disciplina de Pneumologia, Departamento de Clínica Médica, Faculdade de Ciências Médicas, Universidade Estadual de Campinas – Unicamp – Campinas (SP) Brasil.
2. Programa de Pós-Graduação em Ciências da Cirurgia, Faculdade de Ciências Médicas, Universidade Estadual de Campinas – Unicamp – Campinas (SP) Brasil.
3. Disciplina de Medicina Interna e Semiologia, Departamento de Clínica Médica, Faculdade de Ciências Médicas, Universidade Estadual de Campinas – Unicamp – Campinas (SP) Brasil.
4. Departamento de Patologia Clínica, Faculdade de Ciências Médicas, Universidade Estadual de Campinas – Unicamp – Campinas (SP) Brasil.
a. http://orcid.org/0000-0002-2148-5479; b. http://orcid.org/00000-0002-2920-2162; c. http://orcid.org/0000-0003-0742-8846;
d. http://orcid.org/0000-0002-7195-0404; e. http://orcid.org/0000-0002-0539-4243

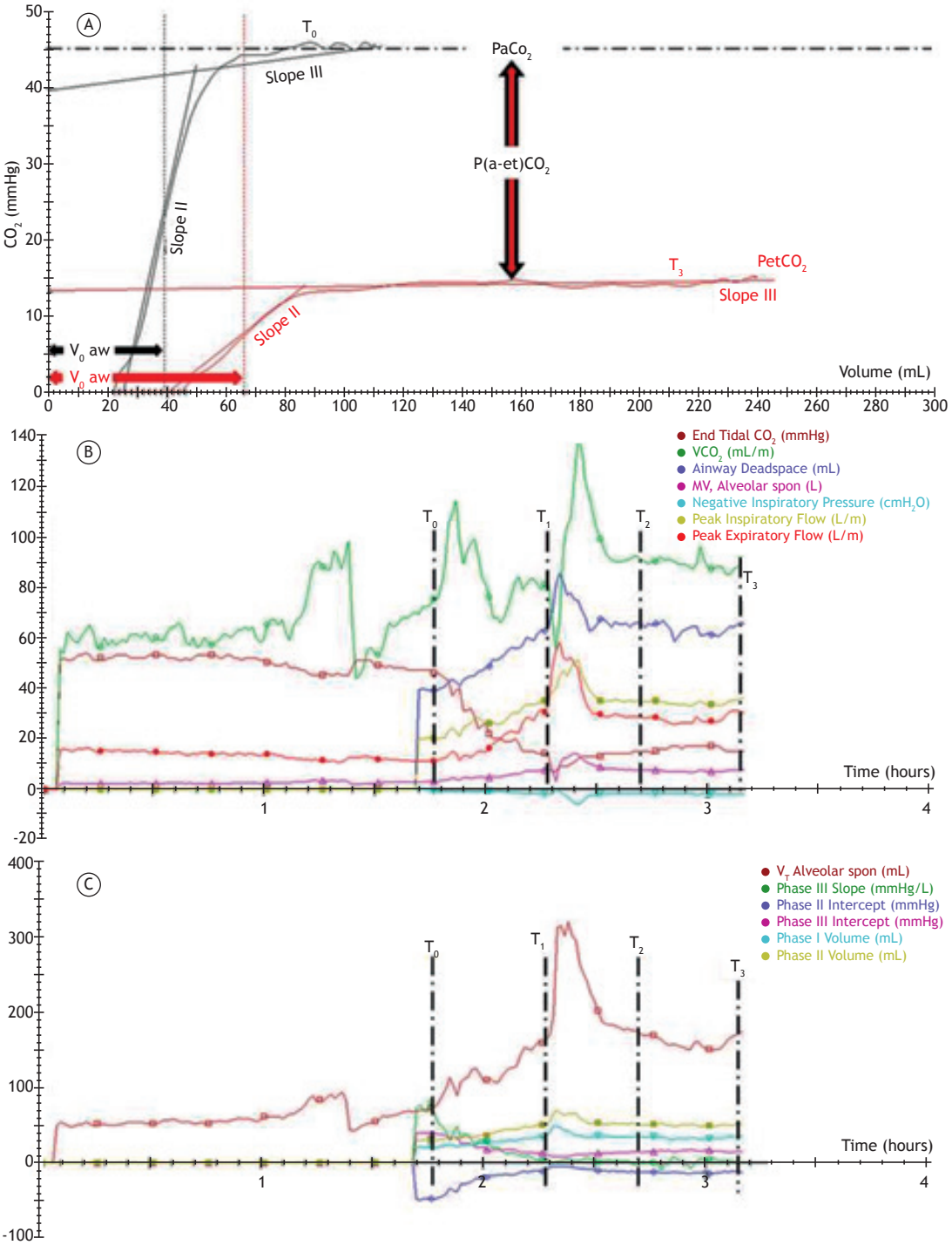

Figure 1. A: representative curves of the volumetric capnography (volume × CO_2) at baseline (T_0, black) and at 1 h after the endpoint (T_3, red). B and C: representative curves of trends seen throughout the experiment. Figures obtained and adapted from the Analysis Plus software (Novametrix, Wallingford, CT, USA). T_0: baseline; T_1: endpoint; T_2: 30 min after T_1; T_3: 1 h after T_1; V_0 aw: anatomical dead space volume; End-Tidal CO_2: end-tidal expiratory pressure of CO_2; VCO_2: CO_2 production (mL/m); Airway dead space: anatomical dead space volume; MV, Alveolar spon: spontaneous alveolar minute volume; V_T, Alveolar spon: spontaneous alveolar tidal volume; Phase III Slope: phase III slope of the capnogram; Phase II Intercept: intercept of the phase II slope of the capnogram; Phase III Intercept: intercept of the phase III slope of the capnogram; Phase I Volume: volume of the phase I slope of the capnogram; and Phase II Volume: volume of the phase II slope of the capnogram.

(such as that occurring in bronchiectasis, cystic fibrosis, and COPD).[7,8]

It was necessary to normalize VCO_2/V_{Te}, SII/P_ECO_2, $SIII/P_ECO_2$, $SIII/PetCO_2$, and $SIII/V_{Te}$, in order to allow

Table 1. Respiratory mechanics, gas exchange, and hemodynamic variables.

Variable	Time point				
	T_0	T_1	T_2	T_3	p
RR (breaths/min)	47 ± 9	48 ± 8	53 ± 11	54 ± 12	0.061
MValv (L)	4.0 ± 0.9	10.6 ± 2.9	9.9 ± 3.8	7.8 ± 1.6	< 0.0001
VDalv (L)	2.4 ± 0.6	4.0 ± 0.8	4.1 ± 1.4	3.8 ± 1.1	< 0.0001
$PetCO_2$ (mmHg)	40.1 ± 2.0	11.0 ± 2.7	16.9 ± 5.5	19.7 ± 4.6	< 0.0001
VCO_2 (mL/min)	95 ± 23	83 ± 20	126 ± 25	114 ± 27	0.001
VCO_2/V_{Te} (mL/L/min)	0.69 ± 0.10	0.28 ± 0.08	0.49 ± 0.10	0.53 ± 0.10	< 0.0001
VCO_2/V_Talv (mL/L/min)	1.09 ± 0.16	0.40 ± 0.13	0.70 ± 0.16	0.79 ± 0.15	< 0.0001
SII (mmHg/L)	1414.3 ± 232.5	185.1 ± 66.8	330.7 ± 128.4	441.1 ± 125.0	< 0.0001
SIII (mmHg/L)	56.73 ± 11.86	−1.10 ± 1.16	7.93 ± 10.06	13.02 ± 10.22	< 0.0001
SII/P_ECO_2	107.61 ± 33.42	31.15 ± 8.06	38.86 ± 12.09	51.35 ± 12.92	< 0.0001
$SIII/P_ECO_2$	4.247 ± 1.188	−0.185 ± 0.210	0.788 ± 0.898	1.366 ± 0.758	< 0.0001
$SIII/PetCO_2$	1.409 ± 0.247	−0.095 ± 0.108	0.378 ± 0.472	0.603 ± 0.362	< 0.0001
$SIII/V_{Te}$	0.427 ± 0.137	−0.004 ± 0.004	0.031 ± 0.037	0.060 ± 0.043	< 0.0001
Intercept Y2 (mmHg)	−48.7 ± 3.7	−9.5 ± 2.1	−15.0 ± 5.8	−19.2 ± 4.8	< 0.0001
Intercept Y3 (mmHg)	35.8 ± 1.7	11.8 ± 2.1	15.7 ± 4.1	18.2 ± 3.0	< 0.0001
P1V (mL)	28.0 ± 5.1	43.5 ± 5.9	41.5 ± 7.4	38.0 ± 6.0	< 0.0001
P2V (mL)	36.0 ± 5.0	63.0 ± 9.3	59.3 ± 11.4	52.7 ± 8.7	< 0.0001
PFI (L/min)	25.5 ± 3.6	38.7 ± 4.9	38.6 ± 7.7	34.6 ± 3.1	< 0.0001
PFE (L/min)	16.3 ± 3.4	49.2 ± 9.8	39.4 ± 16.2	31.8 ± 9.4	< 0.0001
T_i (s)	0.49 ± 0.06	0.65 ± 0.11	0.57 ± 0.09	0.53 ± 0.12	< 0.0001
T_e (s)	0.85 ± 0.20	0.74 ± 0.26	0.66 ± 0.21	0.65 ± 0.20	0.0348
$PaCO_2$ (mmHg)	44.92 ± 4.44	48.22 ± 5.97	45.37 ± 5.82	43.52 ± 6.21	0.158
$P(a\text{-}et)CO_2$ (mmHg)	4.8 ± 2.8	37.2 ± 5.8	28.5 ± 4.5	23.8 ± 3.5	< 0.0001
DC (L/min)	4.9 ± 1.0	2.7 ± 1.0	3.6 ± 1.1	3.9 ± 1.3	< 0.003

T_0: baseline; T_1: endpoint; T_2: 30 min after T_1; T_3: 1 h after T_1; RR: respiratory rate; MValv: alveolar minute volume; VDalv: alveolar dead space volume; $PetCO_2$: end-tidal CO_2 partial pressure; VCO_2: CO_2 production; V_{Te}: expiratory tidal volume; V_Talv: alveolar tidal volume; SII: phase II slope of the capnogram; SIII: phase III slope of the capnogram; P_ECO_2: partial pressure of CO_2 in exhaled air; Intercept Y2: intersection between SII and the y axis; Intercept Y3; intersection between SIII and the y axis; P1V: volumetric capnography phase 1 volume; P2V: volumetric capnography phase 2 volume; PIF: peak inspiratory flow; PEF: peak expiratory flow; T_i: inspiratory time; T_e: expiratory time; $P(a\text{-}et)CO_2$: arterial to end-tidal CO_2 gradient; and CO: cardiac output.

them to be compared to the equivalent CO_2 excretion rates (P_ECO_2, $PetCO_2$, and V_{Te}, respectively).[9]

Other variables that are not usually described in the literature are intercept Y2 and intercept Y3 (both in mmHg), which indicate an increase or a decrease in the caliber of the conducting airways. These variables refer to the intersection of SII and SIII with the y axis of the VCap curve and represent a mathematical increase of the inclination of the slopes. Scheffzek et al.[10] were able to verify that. In the present study, there was a significant variation in those two variables ($p < 0.0001$ for both).

In conclusion, recording, observing, and analyzing the behavior of the parameters of respiratory mechanics, especially VCap, made it possible to identify MPE. When carefully applied and analyzed, our results can make a major contribution to decreasing morbidity and mortality in patients presenting with a clinical profile suggestive of MPE.

Further studies of MPE, either experimental or clinical, are still needed. Such studies could broaden our knowledge of the disease and of its implications for the cardiopulmonary system.

REFERENCES

1. Ferreira JH, Terzi RG, Paschoal IA, Silva WA, Moraes AC, Moreira MM. Mechanisms underlying gas exchange alterations in an experimental model of pulmonary embolism. Braz J Med Biol Res. 2006,39(9):1197-204.
2. Moreira MM, Terzi RGG, Paschoal IA, Martins IC, Oliveira EP, Falcão AI. Thrombolysis in massive pulmonary embolism based on the volumetric capnography. Arq Bras Cardiol. 2010;95:e97-e99. https://doi.org/10.1590/S0066-782X2010001400025
3. Pereira DJ, Moreira MM, Paschoal IA, Martins IC, Metze K, Moreno Junior H. Near-fatal pulmonary embolism in an experimental model: hemodynamic, gasometric and capnographic variables. Rev Bras Cir Cardiovasc. 2011;26(3):462-8. https://doi.org/10.5935/1678-9741.20110023
4. Moreira MM, Terzi RG, Pereira MC, Grangeia Tde A, Paschoal IA. Volumetric capnography as a noninvasive diagnostic procedure in acute pulmonary thromboembolism. J Bras Pneumol. 2008;34(5):328-32. https://doi.org/10.1590/S1806-37132008000500013
5. Schreiner MS, Ieksell IG, Gobran SR, Hoffman EA, Scherer PW, Neufeld GR. Microemboli reduce phase III slopes of CO2 and invert phase III slopes of infused SF6. Respir Physiol. 1993;91(2-3):137-54. https://doi.org/10.1016/0034-5687(93)90095-R
6. Schwardt JD, Gobran SR, Neufeld GR, Aukburg SJ, Scherer PW.

Sensitivity of CO2 washout to changes in acinar structure in a single-path model of lung airways. Ann Biomed Eng. 1991;19(6):679-97. https://doi.org/10.1007/BF02368076

7. Veronez I, Pereira MC, da Silva SM, Barcaui IA, De Capitani EM, Moreira MM, et al. Volumetric capnography for the evaluation of chronic airways diseases. Int J Chron Obstruct Pulmon Dis. 2014;9:983-9. https://doi.org/10.2147/COPD.S62886
8. da Silva SM, Paschoal IA, De Capitani EM, Moreira MM, Palhares IC, Pereira MC. COPD phenotypes on computed tomography and its correlation with selected lung function variables in severe patients. Int J Chron Obstruct Pulmon Dis. 2016;11:503-13. https://doi.org/10.2147/COPD.S90638
9. Scherer PW, Gobran S, Aukburg SJ, Baumgardner JE, Bartkowski R, Neufeld GR. Numerical and experimental study of steady-state CO2 and inert gas washout. J Appl Physiol (1985). 1988;64(3):1022-9. https://doi.org/10.1152/jappl.1988.64.3.1022
10. Scheffzek S, Mosing M, Hirt R, Iff I, Moens Y. Volumetric capnography curves as lung function test to confirm bronchoconstriction after carbachol challenge in sedated dogs. Res Vet Sci. 2012;93(3):1418-25. https://doi.org/10.1016/j.rvsc.2012.04.010